Spot weld strength determination using the wedge test: in-situ observations and coupled simulations

Rémi Lacroix[1,a], Joël Monatte[1,] Arnaud Lens[2,b], Guillaume Kermouche [3], Jean-Michel Bergheau[3], Helmut Klöcker[1,c]

[1]Ecole des Mines de Saint Etienne, 158 cours Fauriel, 42023 Saint Etienne, France

[2] ArcelorMittal Maizières Voie Romaine, BP30320, 57283 Maizères-les-Metz, France

[3]Université de Lyon, ENISE, LTDS, UMR 5513 CNRS, 58 rue jean Parot, 42023 Saint-Etienne Cedex 2, France

[a]lacroix@emse.fr, [b]arnaud.lens@arcelormittal.com, [c]klocker@emse.fr

Keywords: Spot welds, High Strength Steels, wedge test, in-situ.

Abstract. This paper describes an innovative way to characterize the strength of spot welds. A wedge test has been developed to generate interfacial failures in weldments and observe in-situ the crack propagation. An energy analysis quantifies the spot weld crack resistance. Finite Element calculations investigate the stresses and strains along the crack front. A comparison of the local loading state with experimentally observed crack fronts provides the necessary data for a failure criterion in spot weld fusion zones. The method is applied to spot welds of Advanced High Strength steels.

Introduction

New steels are continuously developed in order to reduce the weight of cars, and thus their fuel consumption. The main technology used to assemble these steels is resistance spot welding. The recent development of Advanced High Strength (AHS) steels has made the determination of their weldability a crucial industrial issue. The Cross Tensile (CT) test, illustrated in figure 1.a, is widely used to evaluate the weldability of steel grades. During the CT test a crack propagates from the notch towards the weld nugget (figure 1b). Crack deviation leads to the formation of a plug. The acceptability of spot welds after CT test has been empirically related to a minimum plug diameter so defining an acceptability criterion [1] in the case of mild steels.
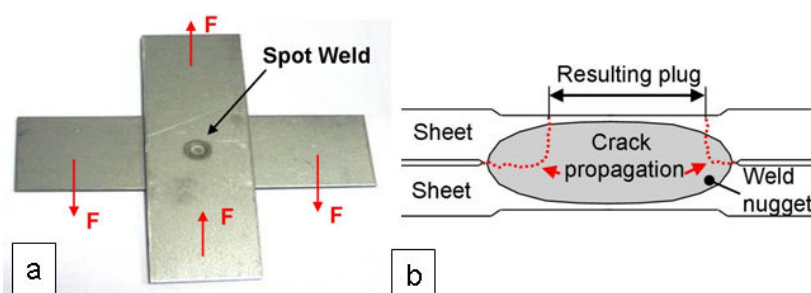

Figure 1 – (a) a spot weld and the CT test configuration, (b) a schematic representation of a cross section of weld with the resulting plug after failure.

The theoretical strength of spot welds in AHS steels submitted to the CT test has been frequently studied [2,5]. However, the experimental results of Oikawa et al [6] show that the CT-test does not lead to reproducible results for AHS steels. Moreover, experimental studies by Nait Oultit et al. [7] have highlighted inconsistencies in using the minimum plug diameter as an acceptability criterion for AHS steels. This criterion has been rejected for AHS steels by the World Auto Steel Guidelines [8].

In this study, we aim at obtaining reproducible data on the local stress and strain fields in the weldment, and at reliably quantifying the fracture properties of fusion zones. A test highlighting the properties of the fusion zone rather than the rest of the weld assembly has been developed. Reproducible fracture of the weldment through the interfacial plane has been achieved by a wedge test. The energy release rate during crack propagation has been quantified by a macroscopic analysis. A local analysis of the crack front correlated with a Finite Element model of the test investigates stresses and strains at failure. More generally the fracture properties of the fusion zone determined in this work are useful for structural integrity calculations of welded assemblies.

The Wedge Test

The Wedge Test is developed in order to allow in-situ observation of crack propagation in the weldment. It also implies an interfacial failure under limited sheet bending, such that most of the energy is used to fracture the weld rather than bend the sheets. This paragraph describes the mechanical set up of the test, the instrumentation and the automatic processing of the in-situ observations.

The test is developed for welded sheets of 2 mm thickness. A wedge test sample is obtained by cross-sectioning a spot weld, as specified on figure 2.a. The sample thus exhibits two notches and a microstructure ranging from the base material to the fusion zone, as shown in the micrography on figure 2.c. This cross section surface will be observed during the wedge test. Cross sectioning is not made exactly in the weld median plane, but is slightly offset to leave a small joint between the sheets.

One side of the sample is clamped, and a 90° wedge is driven in between the welded sheets on the opposite side, as shown in figure 2.d. The wedge is pushed along the interfacial plane of the weld assembly.
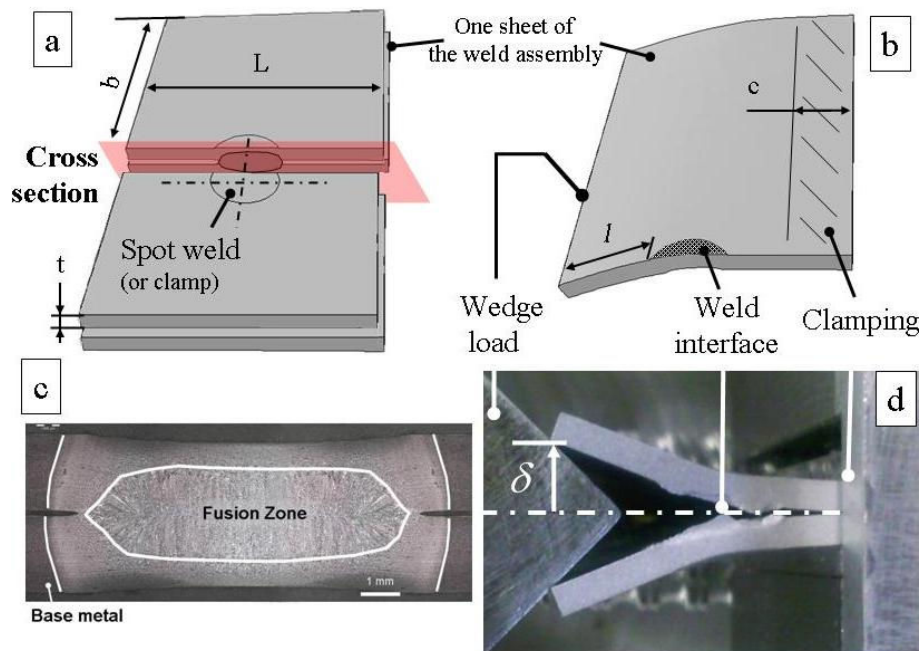

Figure 2 – (a) The wedge test sample sectioning (L=30 mm, b=40 mm, t=2mm, l=7mm, c=10 mm) (b) Mechanical loading of one sheet of the weld assembly. (c) A DP780 spot weld micrography highlighting the main weldment zones, and (d) mechanical set up of the wedge test.

The clamping ensures that the sample interface is parallel to the direction of the wedge displacement. A brushless motor applies a wedge speed of 0.01 mm/s. On the wedge crosshead guide, a Linear Variable Differential Transformer (LVDT) sensor measures the applied displacement, and a load cell records the applied load up to 10kN.

The clamping and the weld interface induce bending of one sheet of the weld assembly with a non-uniform lever arm during the wedge load, as illustrated in figure 2.b.

The weld cross-section is observed by a CDD camera which records 1280x1024 pixels grey images at a frame rate of 2s-1. A 12.5:1 optical system allows the observation of a zone of 5.5x4.4 mm². The observed surface is previously sand blasted in order to generate a speckle-like pattern, of average diameter 30µm. The recording process has been developed with the LabVIEW TM software, and simultaneously acquires the load and displacement with the associated image of the observed surface.

A Digital Image Correlation software developed in-house gives the displacement field between successive images. The crack tip is continuously located by fitting the local displacement field for zero vertical displacement. The accuracy of this measurement is 15 pixels, or 65 µm.

Local quantification of the crack resistance of the weld requires a knowledge of the complete crack front profile. Surface observation on the cross section however gives very limited information on the crack front. The complete crack front profile has been observed on samples partially fractured by interrupted Wedge Tests. These samples were later fully fractured under liquid nitrogen cooling, such that a brittle failure occurs in the remaining joint. The profile of the crack front after the interrupted wedge test is the limit between the all-brittle zone and the mixed (brittle and ductile) zone. The limit between both zones can be easily observed by SEM.

Fracture analysis

Various studies of the wedge test have produced macroscopic analyses of the test, particularly in adhesive [9,10] or brazed joints [11]. However, these tests are all close to a two dimensional configuration, and well suited to an elastic Double Cantilever Beam (DCB) analysis, as described by Kanninen [12]. The variation of the local loading state along the crack tip is neglected in most studies [9,11]. In the case of spot welds, the wedge test has a fully three dimensional geometry. A macroscopic analysis of the wedge test is first investigated, and then a 3D FE analysis is carried out to investigate the stresses and strains along the crack front.

Macroscopic analysis. A macroscopic analysis of the wedge test is based on the load - displacement curve. Figure 3.a illustrates these data recorded for a spot weld of Dual Phase 780 (DP780) steel. The spot welds are loaded in 4 successive cycles. The displacement $u_{start}^{(i)}$ at the beginning of the ith cycle gives information about the energy dissipated during the previous cycles (1,..i-1). We assumed in this study that this energy is dissipated only in the sheet plastic bending and in the weld failure.

The elastic energy $W^{e(i)}$ stored in the sample during cycle (i) can be determined from the load - displacement curves. The linear part of the loading cycle n° i gives $W^e(i)=P.(u_{end}^{(i)}-u_{start}^{(i)})/2$, P and $u_{end}^{(i)}$ being the load and displacement at the end of the linear behaviour, $u_{start}^{(i)}$ the displacement at the beginning of the linear behaviour, as illustrated on the figure 3.a for one cycle. Assuming a linear evolution of the displacements u_{start} between the measured locations for two cycles ($u_{start}^{(i)}$ and $u_{start}^{(i+1)}$) it is possible to estimate W^e for any displacement u of the wedge : $W^e(u)=P(u-u_{start})/2$.
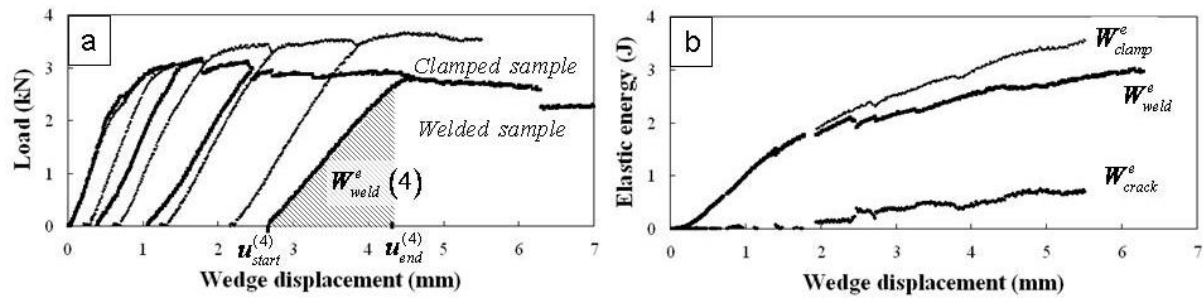
Figure 3 – (a) Load - displacement curve for repeated loading of a DP780 spot weld, and for clamped DP780 steel sheets. The hatched area corresponds to the elastic energy. (b) Elastic energy stored in these two samples.

In a second test, the (elastic) energy (W^e_{clamp}) stored during deformation of the sample without crack propagation is determined. A specific sample made out of the same material with the same geometry is used. One bolt clamps two steel sheets in the same manner as the weld interface joins the sheets in the welded sample. A comparison of the energy W^e_{clamp}, stored in the sample without crack propagation, with that of the energy in the sample with crack propagation (W^e_{weld}), allows an estimation of the energy released during crack propagation (W^e_{crack}).

This analysis neglects some small sliding between the clamping bolt and the sheets. Figure 3.a shows a typical result of this test. W^e_{crack} is thus estimated by $W^e_{crack} = W^e_{clamp} - W^e_{weld}$, as illustrated in figure 3.b.

Finite Element analysis. The FE model of the Wedge Test has been carried using standard ABAQUS according to the procedures described in the manual [13], and is shown in figure 4. This model investigates the stresses and strains along the crack front before propagation, as crack propagation is not yet implemented. The weld interfacial plane is a plane of symmetry. Thus only one sheet is studied, assuming it is clamped in the weldment interface and the sample clamping (figure 2.b). The wedge movement into the sample is modelled assuming a frictionless hard contact. The current model is limited to two zones: the base metal and the fusion zone. The latter is extended through the HAZs to meet the base metal zone. The mechanical behaviour of the base metal and the fusion zone have been characterised independently by tensile and compressive tests, as described in [14]. The mesh is made of 7400 C3D20R elements, with an element edge size of about 150 μm at the weld interface.
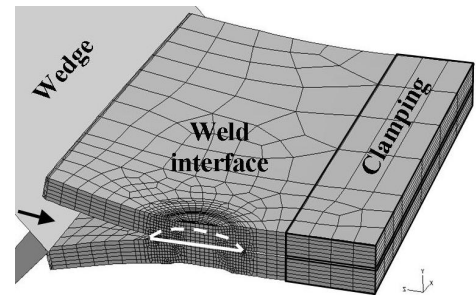

Figure 4 – FE model of the test

Results

The wedge test has been applied to DP780 steel spot welds. Figure 3.a illustrates the load evolution and Figure 5.c the recorded images during a test. The load increases quasi-linearly until a crack appears, and grows up to full interfacial failure. After weld failure, the load drops abruptly and then stays roughly constant during bending of the clamped sheets.

Macroscopic analysis. Figure 5.a illustrates the crack advance based on the in-situ observations, as described above. The crack has advanced 7.4 mm when full interfacial failure occurs, corresponding to the distance between the two notches on the observed surface.
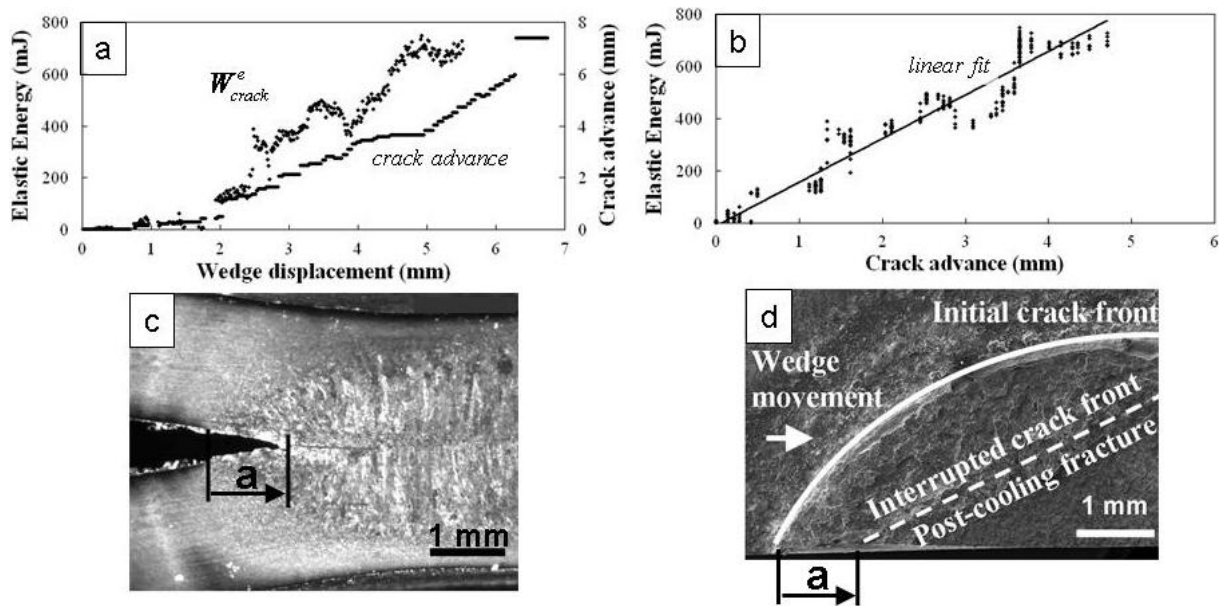

Figure 5 – (a) Crack advance and estimated elastic energy released during crack propagation as a function of the wedge displacement. (b) Estimated elastic energy release as a function of crack advance. (c) In-situ observation of crack advance a. (d) Weld interface after fracture on liquid nitrogen showing the initial and current crack front.

The evolution of the estimated energy W^e_{crack} as a function of the crack advance is plotted in figure 5.a. A linear fit of W^e_{crack} gives an estimate of the derivative dW^e_{crack}/da, the energy release rate on the crack front, as shown in figure 5.b. It is nevertheless very difficult to conclude on the energy release rate per unit crack front length. Considering the geometry of the test, the loading state along the crack front is not expected to be perfectly homogeneous. However, a first order assumption of homogeneity leads to $G = 1/c \cdot dW/da = 34 \ kJ/m^2$, for a crack front length c of 5 mm at crack initiation. This is also equivalent to a mode I toughness $K_{Ic} = \sqrt{G.E} = 84 \ MPa \ \sqrt{m}$, with E the Young modulus of 210GPa.

Stresses and strains along the crack front. Observations of the crack front on an interrupted wedge test are illustrated in the figure 5.c and 5.d. The original circular crack front is shown by the solid line and the interrupted crack front by the dashed line. The latter is straight and makes an angle between 60 and 70 degrees with the direction of wedge movement. The crack front length varies between 0 and 5 mm during crack propagation.

The loading state along the crack front for a wedge displacement of 1 mm has been evaluated by the model. Figure 6.a illustrates respectively the mesh of the model in the weld interface, and figures 6.b, 6.c and 6.d, illustrate the maximum principal stress, the stress triaxiality and the plastic deformation at the weld interface.

A qualitative comparison between the simulated stresses and strains along the original crack front with figure 5.d shows that a failure criterion based on the maximum principal stress would be more consistent with the observed crack propagation, than a deformation based criterion.
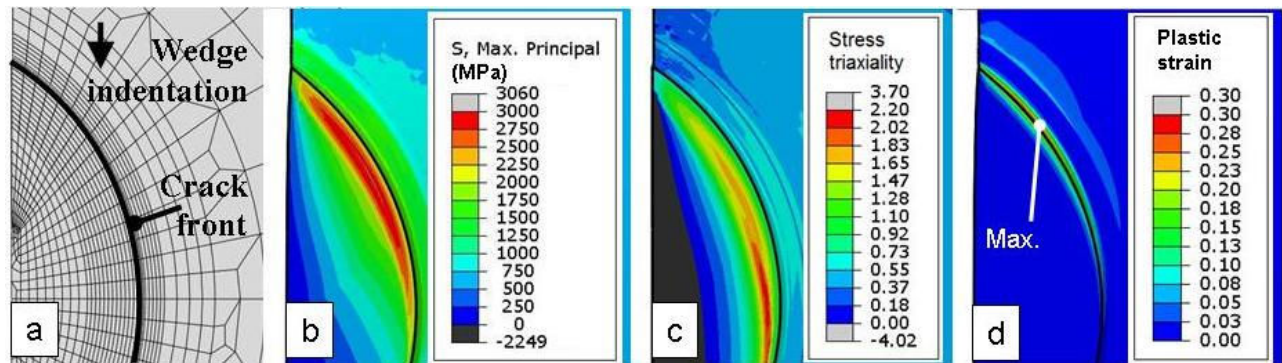
Figure 6 – (a) Mesh of the weld interface. (b) Maximum principal stress, (c) stress triaxiality ratio, (d) equivalent plastic strain in the weld interface.

Conclusions

The wedge test is able to load a spot weld in a quasi-rigid way up to crack initiation and propagation through the weld interface. A simple macroscopic analysis of the test allows the energy released during crack propagation to be estimated. This model has qualitatively shown that a failure criterion based on the maximum principal stress would generate a crack front of a similar profile to the experimentally observed ones.

Further investigations will adapt the FE model to the real crack geometry. The stresses and strains along the evolving crack front during the test could thus be evaluated. The determination of a specific volume of the fracture process zone will finally provide quantitative information for an appropriate failure criterion. The observation of the crack front by means of the interrupted test is a major requirement of this method.

References

[1] NF EN ISO 18278-2, Resistance welding — Weldability.

[2] H Lee, J Choi, Mechanics of Materials 37, 19–32, 2005.

[3] DJ Radakovic, M Tumuluru, Welding Journal 87, 96s-104-s, 2008.

[4] MN Cavalli et al., Fatigue Fract Engng Mater Struct 28, Issue: 10, 861-874, Oct. 2005.

[5] S Dancette et al., New Developments on Metall and Apps of HS steels Buenos Aires 2008.

[6] Oikawa H. et al., Nippon Steel Technical Report No. 95 January 2007.

[7] B Naït Oultit, A Lens, H Klöcker, SMW Conference XIII, AWS Detroit Section, 2008.

[8] AHSS Application Guidelines - Version 3, World Steel Association - September 2006.

[9] J Cognard, J Adhesion 22, 97-108, 1987.

[10] JP Sargent, Int J Adhes Adhes 25, 247-256, 2005.

[11] NR Philips, MY He, AG Evans, Acta Materiala 56, 4593-4600, 2008.

[12] MF Kanninen, Int J Fracture 9, No 1, 83-92, 1973.

[13] ABAQUS, Hibbitt, Karlsson and Sorensen, 2000.

[14] R Lacroix, A Lens, JM Bergheau, G Kermouche, H Klöcker, CFM Conference XIX, 2009.